An E3 ligase TRIM1 promotes colorectal cancer progression via K63-linked ubiquitination and activation of HIF1α

Kun Meng (15896536298@163.com)
https://orcid.org/0000-0002-6541-9510
Liuliu Shi
Xianglan Fang
Lijie Du
Juan Xue
Jin Yang
Yuanjian Hui

Article

Keywords:

Posted Date: November 29th, 2023

DOI: https://doi.org/10.21203/rs.3.rs-3493586/v1

Additional Declarations: There is **NO** conflict of interest to disclose.

Abstract

Accumulating studies have shown that E3 ligases play crucial roles in regulating cellular biological processes and signaling pathways during carcinogenesis via ubiquitination. Tripartite-motif (TRIM) ubiquitin E3 ligases consist of over 70 members. However, the clinical significance and their contributions to tumorigenesis remain largely unknown. In this study, we analyzed the RNA-sequencing expression of TRIM E3 ligases in colorectal cancer (CRC) and identified 10 differentially expressed genes, among which TRIM1 expression predicted poor prognosis of CRC patients. We demonstrated that TRIM1 expression is positively associated with CRC pathological stages, and higher expression is positively correlated with infiltrating levels of immune cells and immunotherapy biomarkers. TRIM1 expression promotes the proliferation and migration of colorectal cancer cells. Transcriptional analysis showed that TRIM1 is responsible for metabolism promotion and immune suppression. Mechanistically, we found that TRIM1 binds HIF1α and mediates its K63-linked ubiquitination, which is required for HIF-1α nuclear translocation and subsequent activation. Our results indicate TRIM1's role in predicting prognosis and immunotherapy efficacy and reveal how TRIM1 functions to upregulate HIF-1α expression and promote tumor cell proliferation.

Introduction

Colorectal cancer is becoming the predominant cancer and the second leading cause of death in cancer patients[1, 2]. It is estimated that about 1.9 million new cases of colorectal cancer worldwide in 2020, of which over 930 000 cases died[3]. Although significant advances in clinical diagnosis, anti-tumor drug discovery and anticancer therapeutics have been achieved, the prognosis remains unoptimistic for lack of the exact molecular diagnosis of CRC. Thus, it is urgent and essential to investigate the molecular mechanisms underlying cancer tumorigenesis and progression, which may be of great significance in developing novel and efficient biomarkers.

Ubiquitination is a highly conserved biological process across eukaryotic organisms and is important for regulating basic cellular processes such as cell cycle, immune invasion, and protein degradation[4]. Three classes of enzymes are involved in this process: the Ub-activating enzyme (E1), the Ub-conjugating enzyme (E2), and the Ub-ligase (E3)[5]. There is increasing evidence that E3 ligase plays a critical role in controlling the development of cancers and is becoming an attractive target for cancer therapies[6, 7]. For example, MDM2 promotes carcinogenesis and metastasis by targeting p53 for proteasomal degradation[8]. SCF^{FBXW7} functions as a tumor suppressor by inhibiting cell cycle progression[9]. The Tripartite-motif (TRIM) ubiquitin ligases are a large family of E3 ligases with over 70 members[10]. However, these proteins' clinical significance and biological functions in cancer remain largely unknown.

In this study, we first identified the differentially expressed TRIM in CRC and their associations with prognosis in CRC. We found TRIM1 was downregulated, and overexpression in CRC was positively associated with poor prognosis and immunotherapy biomarkers. TRIM1 overexpression promotes the

proliferation of CRC cells, facilitates metabolism, and restrains immune response. Mechanistically, TRIM1 interacts with and catalyzes K63-linked ubiquitination of HIF1α, which is required for HIF-1α nuclear translocation and subsequent activation. Our data highlights TRIM1's role in predicting prognosis and immunotherapy efficacy in CRC and reveal its unprecedented functions in regulating tumor cell proliferation.

Results

Landscape of expression pattern of TRIM E3 ligases in human CRC sample

To identify the differentially expressed genes in CRC, we analyzed the RNA-sequencing expression profiles for CRC downloaded from the TCGA dataset (https://portal.gdc.com). A volcano plot showed that 10 TRIMs in CRC samples were differentially expressed, while other TRIMs were unchanged (Figure 1A). Five TRIM expression was significantly upregulated (TRIM14, TRIM15, TRIM24, TRIM29, and TRIM31), and the other five TRIM genes showed decreased expression (TRIM1, TRIM3, TRIM9, TRIM22, and TRIM73) in both colon cancer (COAD) and rectal cancer (READ) (Figures 1A-1B). Interestingly, the downregulated TRIMs and the upregulated TRIMs formed two phylogenetically distinct clusters, indicating their synergistic and divergent roles in CRC cancer development (Figure 1C).

Higher expression of TRIM1 predicts poor prognosis in CRC

To determine the significance of these differentially expressed TRIMs in CRC, we analyzed their associations with the prognostic value of CRC patients. We used the RNA-sequencing expression profiles and corresponding clinical information for CRC from the TCGA dataset. Kaplan–Meier survival curve showed that a high mRNA level of *TRIM1* was significantly associated with poor overall survival (OS) and disease-free survival (DFS) in CRC (Figures 2A-2B). Univariate and multivariate Cox regression analyses exhibited that TRIM1 was an independent prognostic factor (Figures 2C-3D). However, the associations of other TRIMs with survival rates and prognostic values in CRC were not significant (Figures 2A-2D). These results showed that only TRIM1 expression could predict prognosis in CRC, emphasizing its role in CRC tumorigenesis. Hence, we choose TRIM1 for the subsequent investigations.

TRIM1 expression is downregulated in CRC

The expression of TRIM1 was observed to be downregulated in the TCGA dataset (Figure 1). To further verify this, we have provided another three pieces of evidence. An independent CRC cohort (GSE244551) containing normal and cancer tissues was examined. The results showed that TRIM1 expression was significantly upregulated in the normal tissues (Figure 3A). Next, we collected four pairs of clinical samples containing the cancer and their adjacent tissues and found that TRIM1 was also upregulated expressed in the adjacent normal tissues (Figure 3B). In addition, we evaluated the protein expression of TRIM1 in cancer tissues and the adjacent normal tissues of the colon using immunohistochemistry. The results showed that TRIM protein was mainly located around the glandular structure of the lumen and was relatively lowly expressed in CRC tissue (Figures 3C-3D). Besides, we examined the TRIM1

expression profile of *TRIM1* among different cancers in the TGCA cohort using the GEPIA web tool. Compared to the normal tissues, *TRIM1* is downregulated in the six types of cancer, including BLCA, COAD, READ, SKCM, UCEC, and UCS, while upregulated in THYM cancer, suggesting the expression varies among different cancers (Figure 3E).

TRIM1 is positively correlated with clinicopathological parameters and immunotherapy biomarkers of CRC

To explore the potential roles of TRIM1 in CRC development, we next analyzed the relationship between TRIM1 mRNA expression level and its clinical outcomes. We observed positive correlations between the expression level of TRIM1and the CRC tumor stage, the EMT signaling, and two malignant tumor marker genes Ki67 and KRAS, implying that TRIM1 may play a promotive role in CRC tumorigenesis (Figures 4A-4C).

Growing studies have proved that microsatellite instability high MSI status (MSI-H) of mismatch repair deficient (dMMR) gene may predict immunotherapeutic response in CRC. dMMR-MSI-H signatures are typically closely related to the high tumor mutation burden (TMB-H) or immune cell infiltration[11, 12]. To determine the potential role of TRIM in immunotherapeutic response, we performed correlation analyses using the TCGA RNA-seq data of CRC samples. The TRIM1 mRNA level highly correlated with the dMMR-MSI-H signature in CRC samples, including three MMR genes (MSH2, MSH6, and PMS2) and MSI score (Figures 4C-4D). TRIM1 expression had non-significant correlations with TMB but showed positive correlation with infiltrating levels of immune cells (CD8+ T cells, CD4+ T cells, macrophage, neutrophils, and dendritic cells) in CRC (Figures 4E-4F). Consistently, TRIM1 mRNA level had dramatically positive coefficients with the canonical immune checkpoint genes (Figure 4G). Together, these results elucidated the possible role of TRIM1 in regulating immunotherapeutic response in CRC.

TRIM1 promotes cell proliferation of CRC

Clinical analyses implied that TRIM1 played a tumor-promoting role in CRC, so we next examined the biological functions of TRIM1 in CRC cells. We synthesized four pairs of siRNAs for the loss-of-function study and found that the first and the second pairs showed an excellent silencing effect (Figure 5A). Also, for the gain-of-function study, we constructed the functional plasmid pCS2-GFP-TRIM1 for over-expression in CRC cells (Figure 5B). Overexpression of TRIM1 in SW480 and LoVo cells dramatically increased the migration rate and the colony formation of CRC cells compared with the corresponding controls (Figures 5C-5F). Silencing of TRIM1 efficiently slowed down the migration rate, decreased the colony number of SW480 cells (Figures 5G-5J), and attenuated the cell proliferation both in SW480 and LoVo cells (Figures 5K). Notably, this inhibition effect was not due to cell death because TRIM1 siRNA treatment did not induce apparent cell death based on the detection of the lactate dehydrogenase (LDH) release and the caspase-3 activity with or without the treatment of the apoptosis stimuli cisplatin (Supplementary Figure 1). Collectively, the above data demonstrated an oncogenic role of TRIM1 in CRC.

TRIM1 facilitates metabolism and restrains immune response

Our results indicate TRIM1 as an essential factor in promoting the proliferation of CRC cells. To investigate the crucial roles of TRIM1 in genome-wide gene expression changes and intracellular signaling pathways, we conducted a systematically transcriptional analysis of TRIM1-transfected SW480 cells was performed. Based on the RNA-seq analyses, TRIM1 transfection in SW480 cells led to the upregulation of 736 genes and the downregulation of 961 genes (Figure 6A). These DEGs were assigned to GO/KEGG analyses, and the top 20 enriched pathway lists were shown. The functions were primarily divided into positive regulation of metabolism (in red) and negative regulation of innate immune (in blue) (Figure 6B, Supplementary Figures 2). The heat map showed the upregulation of critical metabolic genes and the downregulation of immune-related genes (Figure 6C).

To verify the roles of TRIM1 in the negative regulation of inflammation *in vitro*, we examined the canonical NF-κB pathway by NF-κB-luciferase assay and immunoblotting. We found that TRIM1 over-expression in SW480 significantly decreased the TRAF2/TRAF6-mediated NF-κB activity (Figure 6D). Conversely, TRIM1 silencing by siRNA oligonucleotides results in an elevated NF-κB activity (Figure 6E). Besides, TRIM1 knockdown increased the endogenous level of NF-κB phosphorylation and IκBα degradation induced by TNF, confirming the TRIM1-mediated NF-κB pathway blockade (Figure 6F-6G).

TRIM1 interacts with and catalyzes K63-linked ubiquitination on HIF1α

To further understand the molecular mechanism underlying the signaling pathways related to TRIM1 in CRC, we next analyzed the direct Protein interaction network (PPI) to determine potential interaction baits of TRIM1 (also called MID2). Besides the well-studied microtubule-binding protein MID1 and the ubiquitin-conjugating enzyme E2 D4 UBE2D4, we were surprised to find that TRIM1 was closely associated with the transcription factor hypoxia-inducible factor-1α (HIF1α) (Figure 7A). Coimmunoprecipitation (Co-IP) assay showed that TRIM1 and HIF1α could interact with each other (Figures 7B-7C). Also, TRIM1 was observed to co-localize with HIF1α at microtubules by confocal microscopy (Figures 7D). TRIM1 is an E3 Ub ligase, and we next evaluated whether TRIM1 ubiquitinated HIF1α *in vivo*. Compared with the control plasmid, co-transfection of TRIM1 with HIF1α results in robust ubiquitination of HIF1α (Figures 7E). Besides, we used a series of lysine mutants of Ub to determine the poly-Ub chain type on HIF1α. Strong ubiquitination of HIF1α appeared in reactions containing wild-type (WT), K11R, K27R, K29R, K33R, or K63-only Ub (a mutant in which all Lys residues have been mutated to Arg residues except for Lys63). However, in the sample with the K63R or K48-only ubiquitin mutant, ubiquitination was largely inhibited (Figure 7F). Thus, our data suggested that TRIM1 interacted with HIF1α on microtubules and accelerated its K63-conjugated ubiquitination.

TRIM1 promotes HIF1α activity by accelerating its nuclear translocation

Upon activation, the transcription factor HIF1α is translocated into the nucleus and binds the consensus HREs (hypoxia-responsive element) in the target gene promoter regions to initiate expression[13]. Then, we sought to determine the consequences of HIF1α ubiquitination by TRIM1. To mimic the HIF1α activity *in vitro*, we applied an HRE-luciferase reporter. TRIM1 over-expression significantly elevated the HRE activity

(Figure 8A). Conversely, TRIM1 knockdown by siRNA oligonucleotides results in an attenuated HRE activity induced by DMOG (a HIF1α activator) (Figure 8B). Knockdown of HIF1α significantly decreased HRE activity induced by TRIM1 and DMOG (Figures 8C-8D). Besides, our transcriptome results showed the increased expression of HIF1α-downstream genes in the TRIM1-transfection sample (Figure 8E), confirming TRIM1-mediated HIF1α activation. Although several E3 ligases have been reported to regulate HIF1α's activity via alteration of its expression level or protein stability, our results showed that over-expression of TRIM1 did not alter the *HIF1a* mRNA level (Figure 8E). Chase experiments with cycloheximide (CHX) showed that TRIM1 expression also did not affect the protein stability of HIF1α (Figures 8F-8G). Interestingly, TRIM1 overexpression led to the nucleus translocation of endogenous HIF1α (Figures 6H-6I) after nucleus and cytoplasmic fractionation. DMOG and 2-Me(OE)2 were used as the positive and negative controls, respectively. These results suggest that TRIM1 activates HIF1α signaling by accelerating its nucleus translocation instead of altering its expression.

Discussion

Increasing evidence has demonstrated that TRIM proteins play crucial roles in regulating tumorigenesis[14]. TRIM1 is a special E3 ligase at the microtubule involved in cytokinesis and cell division[15, 16]. Two noteworthy reports have shown that a high level of TRIM1 is related to increased chemoresistance and poor prognosis in breast cancer cells[17, 18]. However, TRIM1's associations with the clinical significance, biological functions, and molecular mechanism in carcinogenesis remain unknown. In this study, we demonstrated that TRIM1 expression is positively associated with CRC pathological stages, and higher expression is positively correlated with immunotherapy biomarkers and poor prognosis. TRIM1 markedly promotes CRC cell migration, proliferation, and colony formation in cultured cells. Combined with a systematically transcriptional analysis, we revealed the involvement of TRIM1 in boosting metabolism and inhibiting immune response. Mechanistically, TRIM1 could bind HIF1α to promote its ubiquitination and mediate its nuclear translocation and activation (Figure 6J). Together, our findings provided TRIM1's associations with clinical significance and demonstrated the novel oncogenic role of TRIM1 in CRC via activation of HIF-1α signaling.

Although our data indicates TRIM1 as a cancer-promoting gene, we found that TRIM1 expression is downregulated in tumor tissues of CRC and other four cancer types (Figure 3E). Interestingly, Roy et al. reported that TRIM1 was an immunomodulatory gene. After TNF-α treatment, the mRNA expression and the protein stability were up-regulated[19]. Our study showed that TRIM1 expression is positively correlated with infiltrating levels of immune cells and immune checkpoint genes. We also found that TRIM1 expression negatively regulates the canonical NF-kB. Thus, we speculate that TRIM1 expression may be only induced when the cancer cell receives the immune signals from the tumor immune microenvironment (TIME), thereby contributing to tumor immune escape and sustained tumorigenesis.

HIF1α is important for regulating cellular metabolism and promoting the expression of immunosuppressive factors during tumor development, and its signaling and stability are tightly

controlled by a series of E3 ligases and deubiquitinating enzymes (DUBs) [20-22]. Besides TRIM1, other examples of HIF1α ubiquitination by alternative E3s are VHL[23], TRAF6[24], and recently STUB1[25]. VHL, and STUB1 could mediate K48-linked modification and proteasomal-mediated degradation of HIF1α. Deubiquitinases USP14, USP20, and UCHL1 diminish these effects through their deubiquitination activity. In addition, TRAF6 induces K63 conjugation to HIF1α and maintains HIF1α stability. HIF1α could also be ubiquitinated via K63 linkage by STUB1 independent of oxygen, which is recruited to LAMP2 for CMA-mediated degradation. In this study, we show that K63-linked ubiquitination by TRIM1 is likely to activate HIF-1α signaling by promoting its nuclear translocation instead of influencing the expression level, expanding the role of ubiquitination in HIF1α-signaling regulation. However, the ubiquitination sites of HIF-1α by TRIM1 are not determined in this study.

Microtubule stabilization promotes HIF1α' nucleus translocation under hypoxia(26), but the exact molecular mechanisms remain unknown. A previous study reported that the microtubule-associated motor protein dynein interacts with HIF1α and facilitates HIF1α nucleus translocation. It is proposed that dynein-HIF1α recruits BICD and the nuclear pore complex (NPC) protein RANBP2 to mediate the cargo nucleus translocation[26]. TRIM1 locates on microtubules and contributes to the microtubule stabilization. In this study, we observed TRIM co-localized with HIF1α on microtubules and mediated its K63-linked ubiquitination. K63-linked ubiquitination is reported to be able to act as a scaffold for the formation of large protein complexes. Thus, we speculate that the TRIM1-mediated ubiquitination enhances the formation of cargo complexes of HIF1α with its translocation regulation factors, thus promoting nucleus translocation.

In conclusion, this study provides original data elucidating TRIM1's role in predicting prognosis and immunotherapy efficacy and the possible mechanism of TRIM1 in promoting CRC cell proliferation, making TRIM1 a novel clinical biomarker and promising therapeutic target.

Materials And Methods

Sample Collection

This study was approved by the ethics committee of the Taihe Hospital Affiliated of Hubei University of Medicine. A total of 4 paired CRC specimens (including tumor tissue and the matched normal tissue) and 6 paired paraffin-embedded tissue sections were provided by the Department of Pathology, Taihe Hospital Affiliated.

Plasmids, antibodies, and reagents

For transient expression in mammalian cells, full open reading frames (ORF) for TRIM1 and HIF1α were amplified using a SW480 cDNA library and inserted into the pCS2-EGFP and pCS2-Flag vectors. pRK5-HA-Ub-WT and the lysine mutants plasmids were maintained in our lab[27]. HRE-luc, pNF-κB-Luc, and pRL-TK reporter plasmids were purchased from Addgene. The sequences of all plasmids were confirmed by sequencing before use.

Antibodies for GAPDH (G9545) and Flag (F7425) were purchased from Sigma-Aldrich. EGFP (sc8334) antibody was obtained from Santa Cruz Biotechnology. Antibodies for HIF1α antibodies (D1S7W, #36169S), NF-κB p65 (D14E12, #8242), phospho-NF-κB p65 (Ser536) (93H1, #3033) and IκBα (44D4, #4812) were from Cell Signaling Technology. Anti-TRIM1/MID2 (68359-1-Ig) and anti-HA Epitope Tag (901501) antibodies were from Proteintech and Biolegend. DMOG and 2-ME$(OE)_2$ was from Selleckchem. Cell culture products were from Invitrogen. The relevant chemicals in this study were obtained from Sigma-Aldrich unless stated otherwise.

Cell culture, transfection, and luciferase reporter assay

SW480 and LoVo cells were purchased from the American Type Culture Collection (ATCC). They were cultured in high-glucose Dulbecco's modified Eagle Medium (DMEM, HyClone) supplemented with additional 10% fetal bovine serum (FBS, Gibco), 2 mM L-glutamine, 1% v/v penicillin/streptomycin. Cells were cultured in a humidified incubator with 5% CO2 at 37 °C. Transient transfection reaction was conducted with the Jetprime reagents (Polyplus) according to the manufacturers' data sheets. For the siRNA silencing assay, 200 pmol of siRNAs were transfected into 2×10^6 cells. Sense sequences for the effective siRNAs used in this study are displayed as follows: TRIM1 1# 5'-GCAGCTCTGGTGAATCCAT-3', TRIM1 2#: 5'-GGTGAATACTGCT ATGCAT-3', TRIM1 4#: 5'-GCCTACAAATCAGCTCCAA-3', HIF1α 4# 5'-GGGATTAACTCAGTTTGAA- 3', and negative control (NC): 5'-TTCTCCGAACGTGTCACGT-3'. Luciferase activity was measured using the dual luciferase assay kit (Promega) according to the manufacturer's instructions.

Colony formation assay

CRC cells were first transfected with plasmids for 18 h or siRNA for 48 h. Cells from each sample were re-digested with trypsin and were seeded in a 6-well cell culture dish (1000 cells per well). After a 2-week cultivation, cells were fixed with 4% paraformaldehyde (PFA) and subjected to crystal violet staining. The culture medium was refreshed every 5 days during incubation. Clone numbers were determined from three biological replicates.

Cell viability assay

Cell proliferation was determined by the Cell Counting Kit-8 (CCK-8) (#C0038, Beyotime). Briefly, CRC cells were treated with siRNA for 48 h, re-digested with trypsin, seeded into 96-well plates at a density of 1000 cells per well, and cultured for a certain time. Then, the cells were supplemented with 10 μL CCK-8 and maintained in the incubator for another 2 h. The data was obtained from a microplate reader by measuring the absorbance at 450 nm. For LDH release detection, the culture supernatant was collected for LDH measurement according to the manufacturer's instructions (Cyto-tox96, Promega).
All measurement results were derived from three independent biological triplicates.

Wound scratch assay

Cell migration was determined using the *in vitro* scratch assay. Colorectal cells were cultivated on 6-well plates to approximate 80% confluence. The wound was introduced by scratching with a pipette tip on the monolayer cell. Cells were then gently washed twice with PBS and cultured in a serum-free culture medium. Wound images were captured at the indicated time to calculate the wound width and the closure rate.

Caspase-3 activity assay

Caspase-3 activity was measured as described previously[28]. Briefly, equal volumes of cell lysates were mixed and incubated with reaction buffer (1 M sodium citrate, 10 mM dithiothreitol, and 50 mM Tris-HCl, pH 7.4) containing Ac-DEVD-AFC (20 μM final) for 30 min at 37 ℃. Fluorescence signals were collected every 2 min for 1 h at λExc/λEm≈405/510 nm.

Cycloheximide (CHX) Chase Assays

At 18 h after transfection of the indicated plasmids, SW480 cells were treated with 100 μg/ml CHX before lysates were collected at different time points and analyzed by immunoblotting.

Immunoprecipitation

SW480 cells were transfected with 5 μg of plasmids encoding the interested protein when the cell confluency reached approximately 80% in 6-well plates. After 24 hrs, the cells were washed once with PBS and subsequently lysed in the pre-cooled buffer A (Buffer A: 25 mM Tris-HCl, pH 7.5, 150 mM NaCl, 10% glycerol, and 1% Triton X-100, supplemented with a protease inhibitor mixture). The lysates were pre-cleared and were subjected to anti-Flag or anti-GFP immunoprecipitation according to the standard protocol. After four times washes with ice-cold wash buffer, the immunoprecipitates on the beads were eluted and denatured by boiling in the SDS-containing buffer at 95°C for 5 min, followed by standard immunoblotting analysis.

Immunofluorescence staining and confocal microscopy imaging

Immunofluorescence staining was performed following the standard protocols in our lab[29]. Briefly, cell samples were fixed with 4% PFA for 10 min, permeabilized with 0.2% Triton X-100 for 15 min, incubated with 2% bovine serum albumin (BSA) for a 30-min blockade, then incubated with the indicated primary antibody and subsequent Alexa Fluor-labeled secondary antibody (ThermoFisher). Fluorescence images were acquired under the confocal microscope (FV3000RS, Olympus). All image data shown are representative of randomly selected fields from at least five replicates.

Immunohistochemistry (IHC) Assay

The CRC and paired adjacent tissues were prepared into 3 mm paraffin sections. Each sample was subjected to a 10-minute deaffinity antigen retrieval by sodium citrate (pH 6.0), followed by incubation with mouse monoclonal TRIM1 antibody (1:100 dilution) or mouse control IgG

and subsequent horseradish peroxidase (HRP) labeled secondary antibody. Afterward, each section was subjected to staining with DAB reagent and counterstaining with hematoxylin. The immunoreactive score of the section was calculated as described previously[30].

Transcriptomic analysis

SW480 cells were transfected with a plasmid expression GFP-TRIM1 or GFP. After 24 hrs, total RNA was isolated using TRIzol reagent (Invitrogen), and samples were subjected to RNA-seq at Novogene (Beijing, China). The reads were assigned to the genome sequences of *Homo sapiens*. Relative mRNA expression abundance was quantified by measuring the value of FPKM. The gene expression was considered reliable and significantly different only when the thresholds of *p*-value reached $-\log_{10}(p\text{-value}) > 1.3$. Pathway enrichment of these differential expression genes (DEGs) was performed by GO and KEGG analyses using the DAVID online tool (https://david.ncifcrf.gov/).

Bioinformatic Analysis

The GEPIA online database (http://gepia.cancer-pku.cn/index.html) was used to analyze the mRNA expression of TRIMs between tumor and normal tissue and evaluate the associations between TRIM1 expression and prognosis value in CRC patients. TIMER (https://cistrome.shinyapps.io/timer/) was used to assess the associations between TRIM1 expression and immune cell infiltration levels in COAD and READ. GeneMANIA (http://www.genemania.org) was used to predict the potential binding proteins of TRIM1. Home for Researchers (https://www.home-for- researchers.com) was used to evaluate the correlation between TRIM1 expression and immune checkpoint genes, TMB, and MSI scores.

Quantification and Statistical Analysis

Results are presented as mean ± SD (standard deviation) containing at least three biological replicates. Data were analyzed using a student's *t*-test to compare two experimental groups. A difference is considered significant as the following: $*p<0.05$, $**p< 0.01$.

Declarations

Conflict of Interest

All authors declare no conflict of interest.

Author Contributions

K.M. and Y.H. conceived the study. L.S., X.F. L.D. designed and performed the functional experiments. K.M. and J.X. conducted the bioinformatics analyses

J.Y. and J.X. helped in preparing experiment materials. K.M., Y.H. and L.S. analyzed the data and wrote the manuscript. All authors discussed the results, commented on the manuscript, and approved the final

manuscript.

Acknowledgments

We thank members of the central laboratory of Taihe Hospital for helpful discussions and technical assistance. We thank the members of the Biomedical Research Institute of the Hubei University of Medicine for assisting in Confocal microscope operations. This work was supported by the National Natural Science Foundation of China (32200156), Natural Science Foundation of Hubei Provincial Department of Education (D20222104), Cultivating Project for Young Scholar at Hubei University of Medicine (2019QDJZR09), Hubei Provincial Natural Science Foundation (2022CFB934, 2023AFB911), the Foundation of Health Commission of Hubei Province (WJ2023F088), and Clinical-Basic Research Project at Taihe hospital (2021LC+JC007).

Data Availability Statement

The raw sequence data reported in this paper have been deposited in the Genome Sequence Archive in BIG Data Center, Beijing Institute of Genomics (BIG) (https://bigd.big.ac.cn/gsa) under the accession number HRA005825. The data supporting the findings of this study and source data are included in the supplementary data and available upon reasonable request.

References

1. Hossain MS, Karuniawati H, Jairoun AA, Urbi Z, Ooi DJ, John A, et al. Colorectal cancer: a review of carcinogenesis, global epidemiology, current challenges, risk factors, preventive and treatment strategies. Cancers. 2022;14(7):1732.
2. Keum N, Giovannucci E. Global burden of colorectal cancer: emerging trends, risk factors and prevention strategies. Nature reviews Gastroenterology & hepatology. 2019;16(12):713-32.
3. Xi Y, Xu P. Global colorectal cancer burden in 2020 and projections to 2040. Translational oncology. 2021;14(10):101174.
4. Callis J. The ubiquitination machinery of the ubiquitin system. The Arabidopsis Book/American Society of Plant Biologists. 2014;12.
5. Haglund K, Dikic I. Ubiquitylation and cell signaling. The EMBO journal. 2005;24(19):3353-9.
6. Deng L, Meng T, Chen L, Wei W, Wang P. The role of ubiquitination in tumorigenesis and targeted drug discovery. Signal transduction and targeted therapy. 2020;5(1):11.
7. Zou T, Lin Z. The involvement of ubiquitination machinery in cell cycle regulation and cancer progression. International Journal of Molecular Sciences. 2021;22(11):5754.
8. Xian L, Zhao J, Wang J, Fang Z, Peng B, Wang W, et al. p53 Promotes proteasome-dependent degradation of oncogenic protein HBx by transcription of MDM2. Molecular biology reports. 2010;37:2935-40.

9. Galindo-Moreno M, Giráldez S, Limón-Mortés MC, Belmonte-Fernández A, Reed SI, Sáez C, et al. SCF (FBXW7)-mediated degradation of p53 promotes cell recovery after UV-induced DNA damage. The FASEB Journal. 2019;33(10):11420.
10. Ikeda K, Inoue S. TRIM proteins as RING finger E3 ubiquitin ligases. Trim/Rbcc proteins. 2012:27-37.
11. Mei W-J, Mi M, Qian J, Xiao N, Yuan Y, Ding P-R. Clinicopathological characteristics of high microsatellite instability/mismatch repair-deficient colorectal cancer: A narrative review. Frontiers in Immunology. 2022;13:1019582.
12. Lin A, Zhang J, Luo P. Crosstalk between the MSI status and tumor microenvironment in colorectal cancer. Frontiers in immunology. 2020;11:2039.
13. Pezzuto A, Carico E. Role of HIF-1 in cancer progression: novel insights. A review. Current molecular medicine. 2018;18(6):343-51.
14. Huang N, Sun X, Li P, Liu X, Zhang X, Chen Q, et al. TRIM family contribute to tumorigenesis, cancer development, and drug resistance. Experimental Hematology & Oncology. 2022;11(1):75.
15. Gholkar AA, Senese S, Lo Y-C, Vides E, Contreras E, Hodara E, et al. The X-linked-intellectual-disability-associated ubiquitin ligase Mid2 interacts with astrin and regulates astrin levels to promote cell division. Cell reports. 2016;14(2):180-8.
16. Zanchetta ME, Meroni G. Emerging roles of the TRIM E3 ubiquitin ligases MID1 and MID2 in cytokinesis. Frontiers in physiology. 2019;10:274.
17. Luo J, Zeng S, Tian C. MORC4 promotes chemoresistance of luminal A/B breast cancer via STAT3-mediated MID2 upregulation. OncoTargets and therapy. 2020:6795-803.
18. Wang L, Wu J, Yuan J, Zhu X, Wu H, Li M. Midline2 is overexpressed and a prognostic indicator in human breast cancer and promotes breast cancer cell proliferation in vitro and in vivo. Frontiers of Medicine. 2016;10:41-51.
19. Roy M. Study of the Role of TRIM Family Proteins in Regulation of TNFα Mediated NF-κB Pathway: Maharaja Sayajirao University of Baroda (India); 2021.
20. McGettrick AF, O'Neill LA. The role of HIF in immunity and inflammation. Cell Metabolism. 2020;32(4):524-36.
21. Kubaichuk K, Kietzmann T. Involvement of E3 Ligases and Deubiquitinases in the Control of HIF-α Subunit Abundance. Cells. 2019;8(6):598.
22. Günter J, Ruiz-Serrano A, Pickel C, Wenger RH, Scholz CC. The functional interplay between the HIF pathway and the ubiquitin system–more than a one-way road. Experimental Cell Research. 2017;356(2):152-9.
23. Kamura T, Sato S, Iwai K, Czyzyk-Krzeska M, Conaway RC, Conaway JW. Activation of HIF1α ubiquitination by a reconstituted von Hippel-Lindau (VHL) tumor suppressor complex. Proceedings of the National Academy of Sciences. 2000;97(19):10430-5.
24. Sun H, Li X-B, Meng Y, Fan L, Li M, Fang J. TRAF6 upregulates expression of HIF-1α and promotes tumor angiogenesis. Cancer Research. 2013;73(15):4950-9.

25. Vasco Ferreira J, Rosa Soares A, Silva Ramalho J, Pereira P, Girao H. K63 linked ubiquitin chain formation is a signal for HIF1A degradation by Chaperone-Mediated Autophagy. Scientific reports. 2015;5(1):10210.
26. Lee HJ, Han HJ. Role of Microtubule-Associated Factors in HIF1α Nuclear Translocation. Oxygen Transport to Tissue XLI. 2020:271-6.
27. Meng K, Yang J, Xue J, Lv J, Zhu P, Shi L, et al. A host E3 ubiquitin ligase regulates Salmonella virulence by targeting an SPI-2 effector involved in SIF biogenesis. mLife. 2023;2(2):141-58.
28. Li T, Shi L, Liu W, Hu X, Hui Y, Di M, et al. Aloe-emodin induces mitochondrial dysfunction and pyroptosis by activation of the caspase-9/3/gasdermin e axis in HeLa cells. Frontiers in Pharmacology. 2022;13:854526.
29. Meng K, Zhuang X, Peng T, Hu S, Yang J, Wang Z, et al. Arginine GlcNAcylation of Rab small GTPases by the pathogen Salmonella typhimurium. Communications Biology. 2020;3(1):287.
30. Tan G, Lin C, Huang C, Chen B, Chen J, Shi Y, et al. Radiosensitivity of colorectal cancer and radiation-induced gut damages are regulated by gasdermin E. Cancer letters. 2022;529:1-10.

Figures

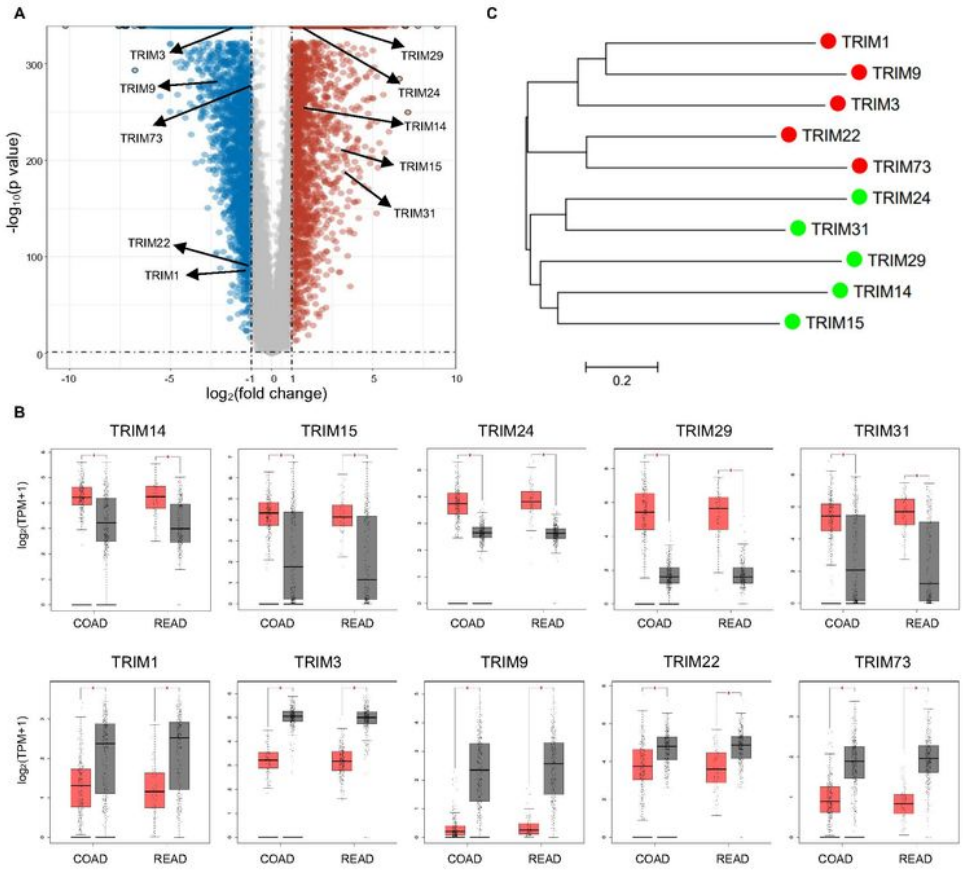

Figure 1

Figure 1

Identification of differentially expressed TRIMs in colorectal cancer.

(A). Volcano map showing the overall transcriptional expression in CRC of tumor tissues (n=620) matching the TCGA data and normal tissues (n=830) matching the TCGA normal and GTEx data. Red

dots refer to significantly up-regulated genes, blue dots correspond to the down-regulated genes, and grey dots indicate the non-significant change in gene expression.

(B). Box plot showing the mRNA expression of differentially expressed TRIMs in COAD and READ of tumor tissues and normal tissues matching the TCGA normal and GTEx data.

(C). Phylogenetic analyses of differentially expressed TRIMs. The amino acid sequence of TRIMs was aligned, and a phylogenetic tree was constructed in MEGA 5.0 using the neighbor-joining method.

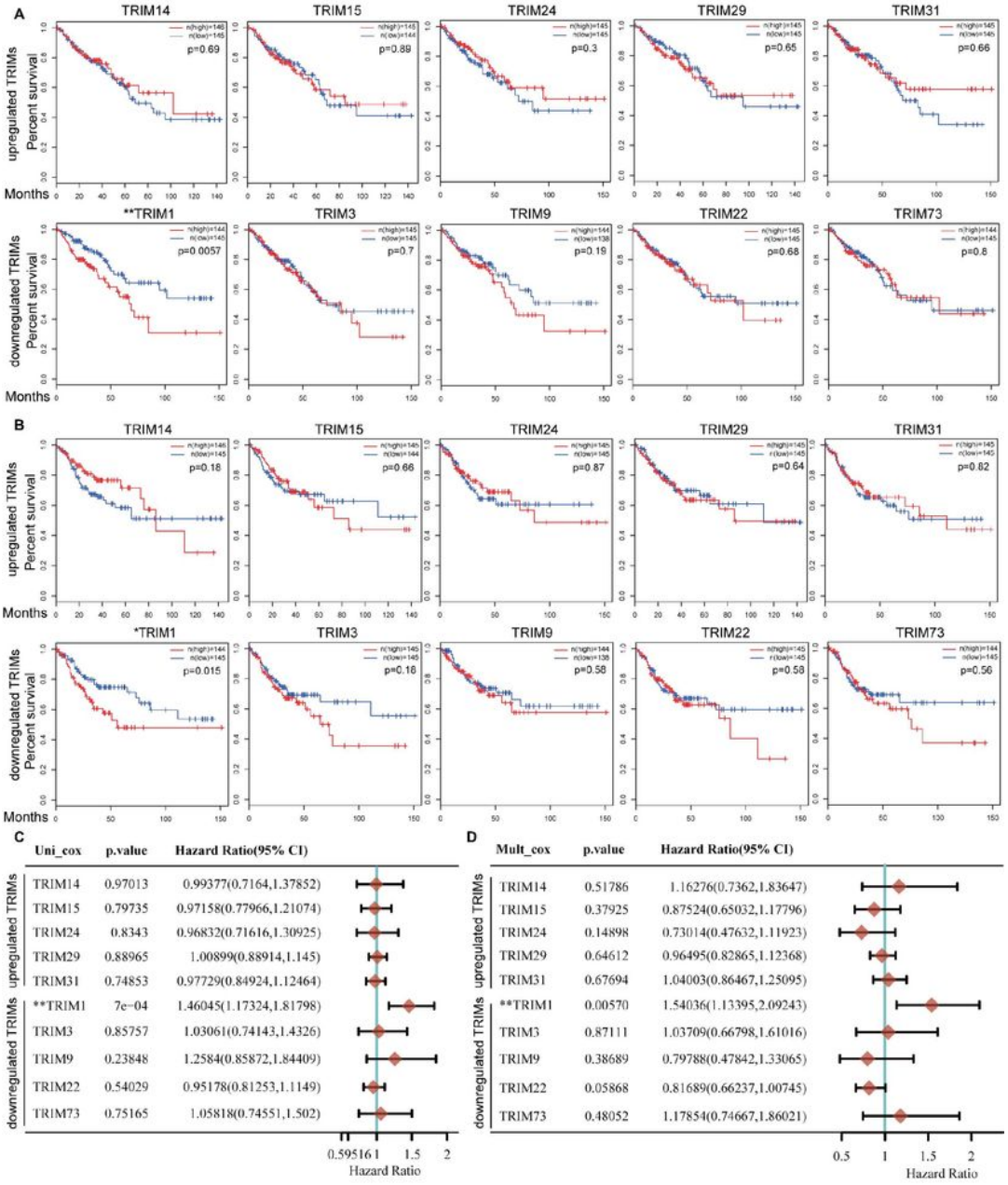

Figure 2

Figure 2

Correlation between *TRIMs* expression and survival rate of CRC patients.

(A-B). Kaplan-Meier plots for the survival of CRC patients stratified by the mRNA expression level of each differentially expressed TRIMs. The overall survival curves are shown in (A). The disease-free survival curves are shown in (B).

(C-D). Cox regression analysis of mRNA expression of each differentially expressed TRIMs in CRC patients from TCGA data. The *p*-value, hazard ratio (HR), and confidence interval of each TRIM in CRC are analyzed by univariate (C) and multivariate (D) Cox regression analysis.

*p<0.05, **p<0.01.

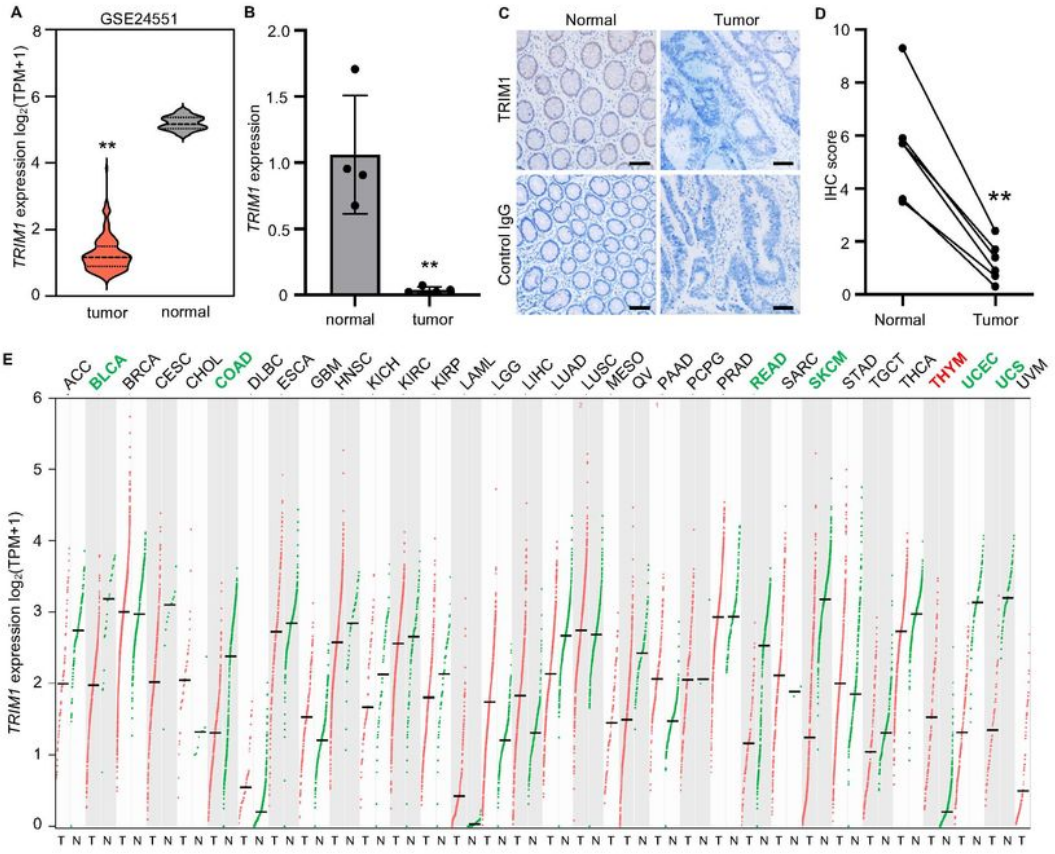

Figure 3

Figure 3

TRIM1 expression is significantly down-regulated in colorectal cancer.

(A) The mRNA expression of *TRIM1* of CRC tumor tissues and their corresponding adjacent normal tissues matching GSE24551 data.

(B) The mRNA expression of *TRIM1* in the tumor tissues compared to the adjacent normal tissues from four CRC patients paired samples.

(C-D) Immunohistochemical staining of TRIM1 protein in paired samples from CRC patients. Representative IHC images of TRIM1 were shown **(C)**, and the IHC scores were calculated **(D)**.

(E) The transcriptional expression profile of *TRIM1* in 33 types of tumor tissues (T) in TCGA and normal tissues (N) matching the TCGA normal and GTEx data. Red and green labels correspond to the cancer types in which *TRIM1* expression is up- and down-regulated in tumor tissue.

Scale bar, 50 μm. *p<0.05, **p<0.01.

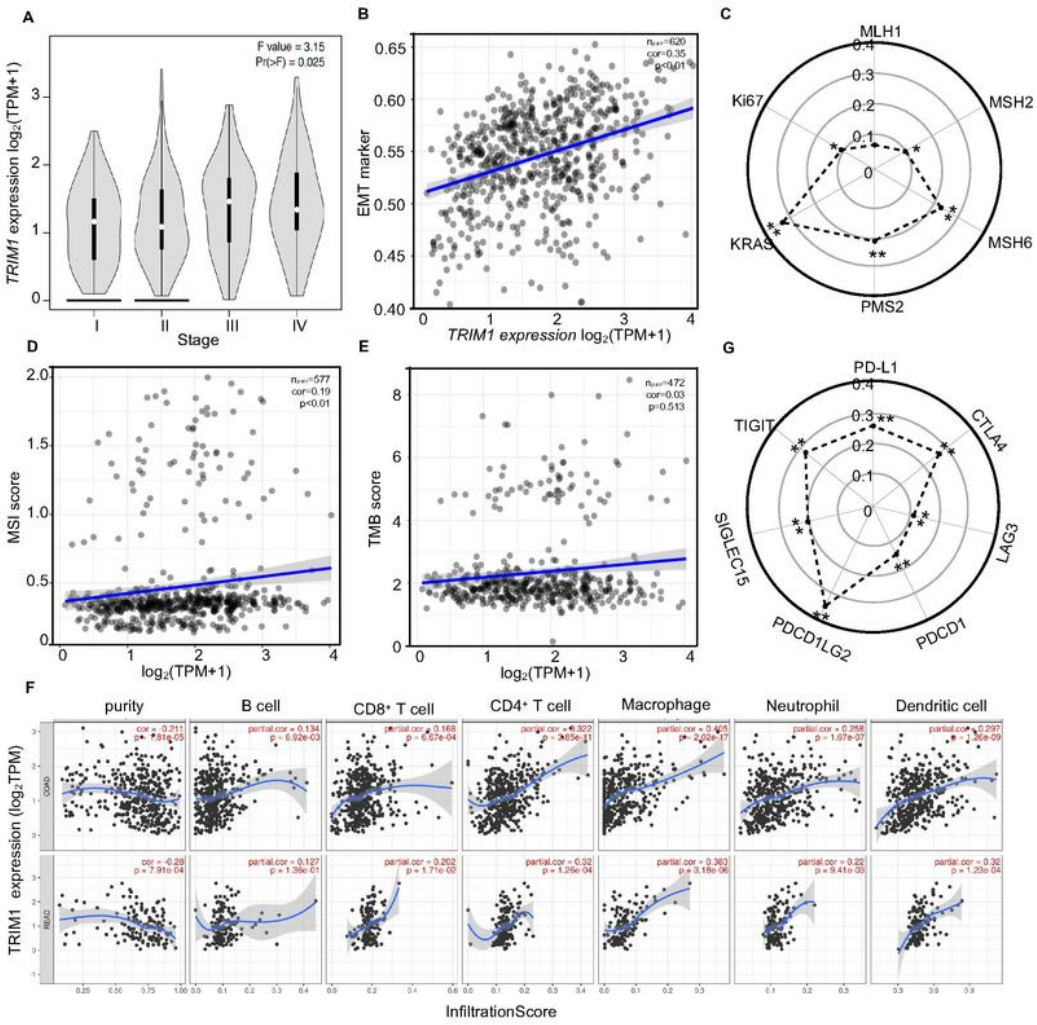

Figure 4

Figure 4

Higher expression of TRIM1 was significantly associated with poor prognostic and immunotherapy biomarkers in colorectal cancer.

(A)TRIM1 expression in different CRC pathological stages using TCGA data.

(B) Correlation between TRIM1 expression and EMT marker by GESA enrichment analysis of CRC patients' data.

(C) Correlation between TRIM1 expression and MMR genes in CRC patients.

(D-E) Correlation analysis between TRIM1 expression and MSI/TMB score of CRC patients. The abscissa represents gene expression distribution, and the ordinate represents MSI **(D)** and TMB **(E)** score distribution. The value in the panel represents the paired-sample number, correlation coefficient, and correlation *p*-value.

(F) Correlation between TRIM1 expression and immune cell infiltration levels in COAD and READ.

(G) Correlation between the TRIM1 expression and immune checkpoint genes.

Spearman's correlation coefficients and *p*-values were shown. *$p<0.05$, **$p<0.01$.

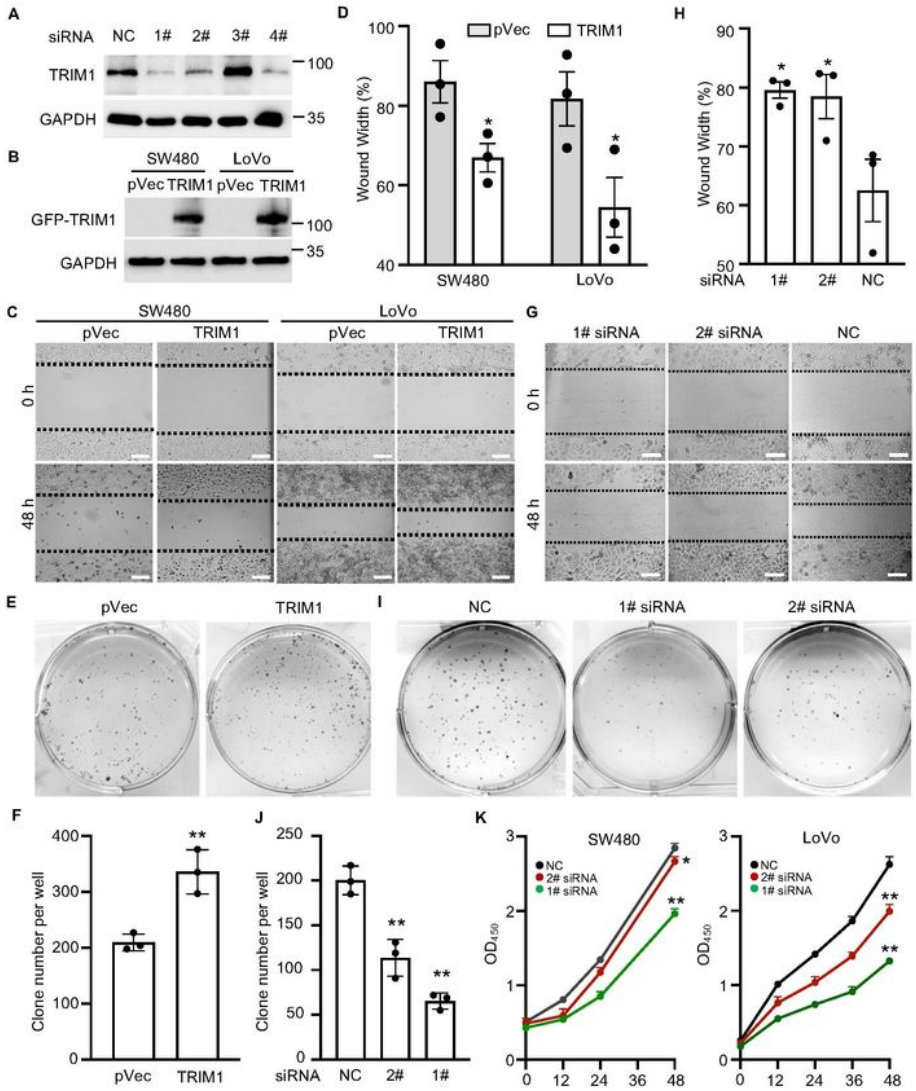

Figure 5

Figure 5

TRIM1 expression promotes the proliferation, migration, and colony formation of colorectal cancer cells. Colorectal cancer cells were transfected with *TRIM1* siRNA for 48 h or transfected with a plasmid expression GFP-TRIM1 or GFP (pVec) for 18 h, and then subjected to wound scratch assay, colony formation assay, or cell proliferation assay.

(A) Knockdown efficiency of *TRIM1* siRNA was detected by immunoblotting.

(B) Over-expressed GFP-TRIM1 protein was detected by immunoblotting.

(C-D) Effects of TRIM1 over-expression on the migration of SW480 and LoVo cells. Representative images were shown **(C)**, and the wound width was calculated **(D)**.

(E-F) Effects of TRIM1 over-expression on the colony formation of SW480 cells. Representative images were shown (**E)**, and the colony number was calculated **(F)**.

(G-H) Effects of *TRIM1* knockdown on the migration of SW480 cells. Representative images were shown **(G)**, and the wound width was calculated **(H)**.

(I-J) Effects of *TRIM1* knockdown on the colony formation of SW480 cells. Representative images were shown (**I)**, and the colony number was calculated **(J)**.

(K) Effects of *TRIM1* knockdown on the cell proliferation of SW480 and LoVo cells.

Results are as means ± SD from three independent experiments. Scale bar, 100 μm. *p<0.05, **p<0.01.

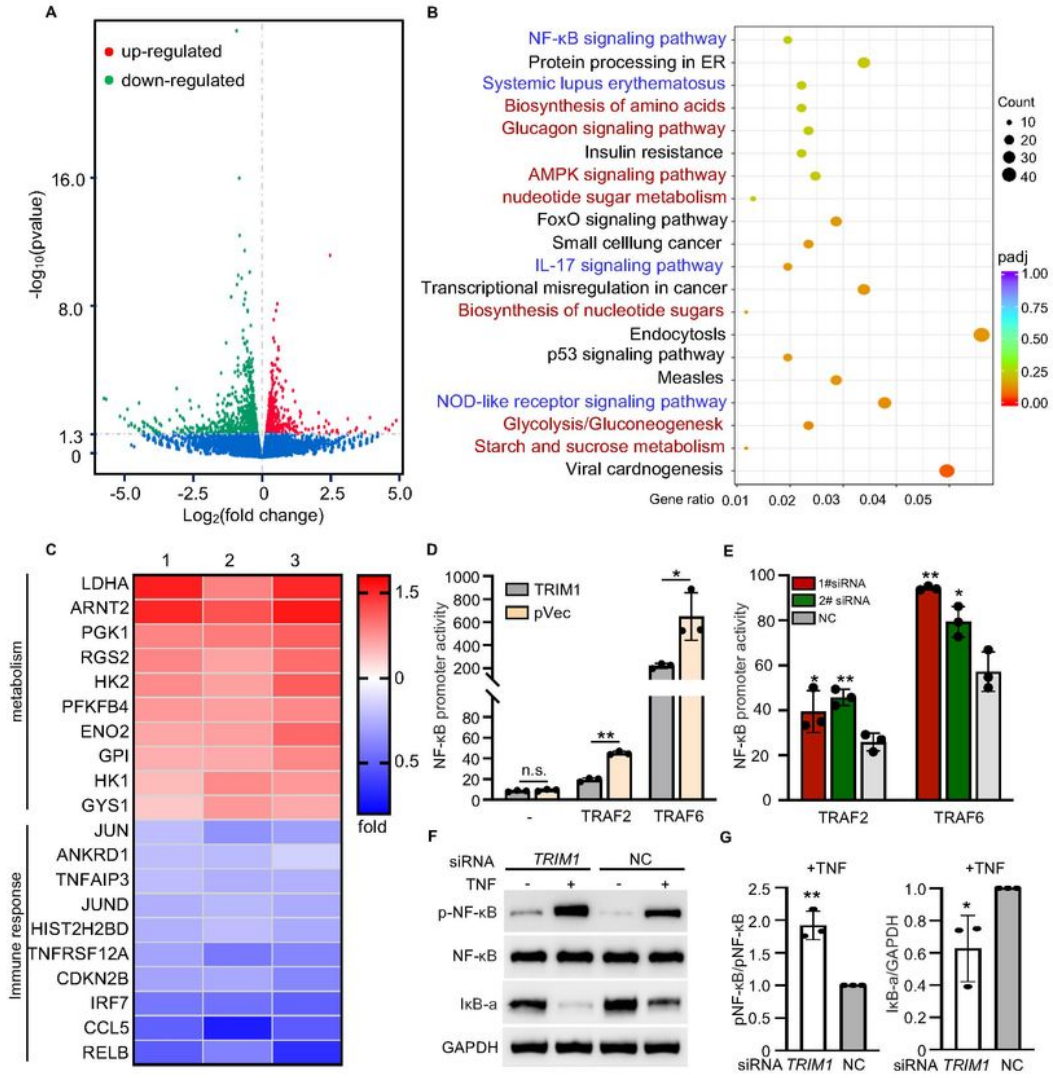

Figure 6

Figure 6

TRIM1 is critical for metabolism promotion and immune suppression.

(A-C) Systematic RNA-seq analysis from TRIM1-overexpressed SW480 cells.

(A) Volcano map showing the overall transcriptional expression in SW480 cells at 18 h post-transfection. Red dots represent the upregulated genes, green dots correspond to the downregulated genes, and blue dots represent insignificant genes.

(B) Pathway enrichment of the DEGs by GO and KEGG analyses using the DAVID online tool. The top 20 pathways were listed. The circle size represents the number of DEGs enriched in this pathway. Red labels correspond to upregulated pathways, and blue labels refer to the downregulated pathways.

(C) Heatmap shows the synergistic expression patterns of the DEGs involved in regulating metabolism and immune response post-TRIM1 transfection. Color change from blue to red represents the expression levels of DEGs from low to high.

(D-E) Effects of TRIM1 overexpression and silencing on the NF-κB activities. **(D)** The plasmid for GFP-TRIM1 or GFP was co-transfected with the plasmid constructs for NF-κB-Luc, adaptor molecule TRAF2 or TRAF6. **(E)**After transfection of TRIM1 siRNA for 48 h, SW480 cells were co-transfected with plasmid constructs for NF-κB-Luc, adaptor molecule TRAF2 or TRAF6 into SW480 cells. NF-κB activity in these samples was determined using the luciferase reporter assay.

(F-G) Effects of TRIM1 knockdown on the NF-κB pathway. After siRNA treatment for 48 h, SW480 cells were added with TNF for another 12 h. **(F)** The expression of NF-κB pathway-related protein was examined by immunoblotting. **(G)**The level of NF-κB pathway activation was quantitated by measuring the ratio of band signal intensity for phosphorylated NF-κB/ total NF-κB, and IκB/GAPDH with Image J. Results are as means ± SD from three independent experiments. *p<0.05, **p<0.01.

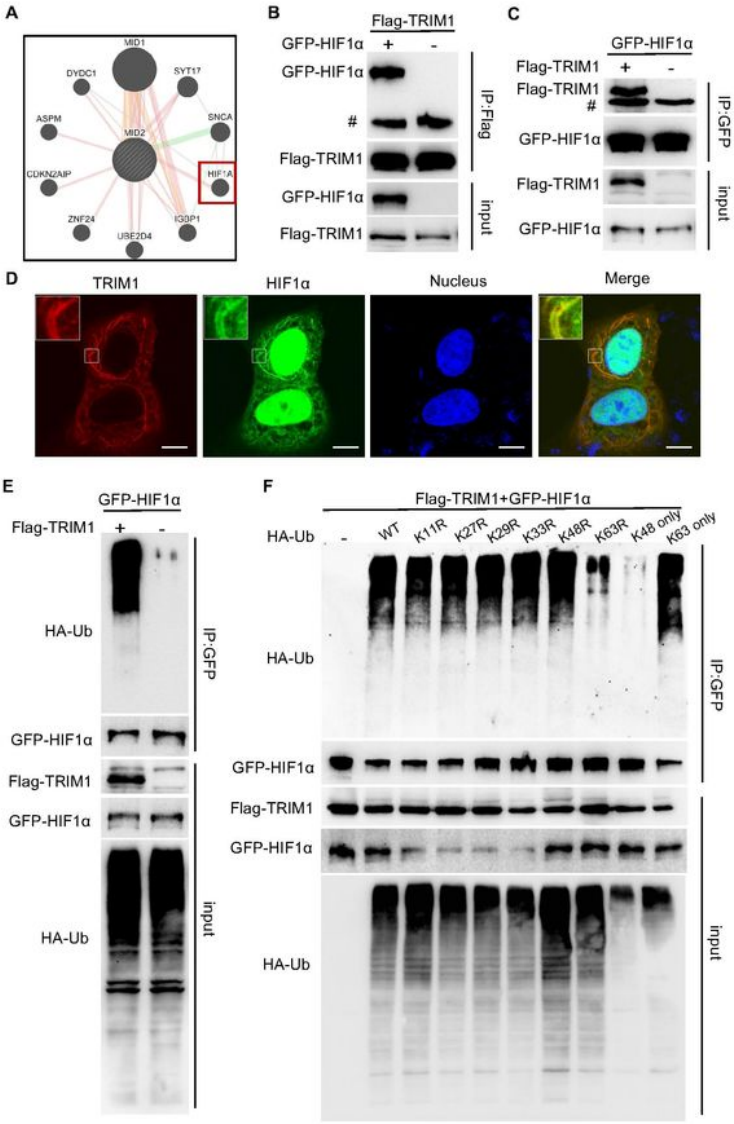

Figure 7

Figure 7

TRIM1 interacts with HIF1α and catalyzes its K63-linked ubiquitination.

(A) The protein-protein interaction network (PPI) of MID2/TRIM1 by GeneMANIA. Shown are the top 10 most related proteins.

(B-C) The interaction between TRIM1 and HIF1α by coimmunoprecipitation (co-IP) assay. SW480 cells were co-transfected with the indicated plasmids. Samples lysed were immunoprecipitated with either anti-Flag or anti-GFP antibody, and the input and immunoprecipitated samples were detected by immunoblotting with the indicated antibodies. **(B)** TRIM1 was co-immunoprecipitated with HIF1α. **(C)** HIF1α was co-immunoprecipitated with TRIM1. # marks the IgG or non-specific protein in the IP blot.

(D)HIF1α co-localized with TRIM1 at microtubules. SW480 cells were co-transfected with GFP-HIF1α and Flag-TRIM1 plasmids for 18 h. Showed are photos of cellular localization of HIF1α (green) and TRIM1 (red). Scale bar, 10 μm

(E-F) Overexpression of TRIM1 promotes K63-linked ubiquitination of HIF1α. GFP-HIF1α expressed-SW480 cells were transfected with Flag-TRIM1 plasmid or the empty control vector in the presence of the WT or the mutated HA-ubiquitin. 18 h post-transfection, GFP-HIF1α was immunoprecipitated with an anti-GFP antibody, followed by immunoblotting analysis with the corresponding antibodies. **(E)** Overexpression of TRIM1 promotes ubiquitination of HIF1α. **(F)** TRIM1 catalyzes K63-linked polyubiquitination of HIF1α.

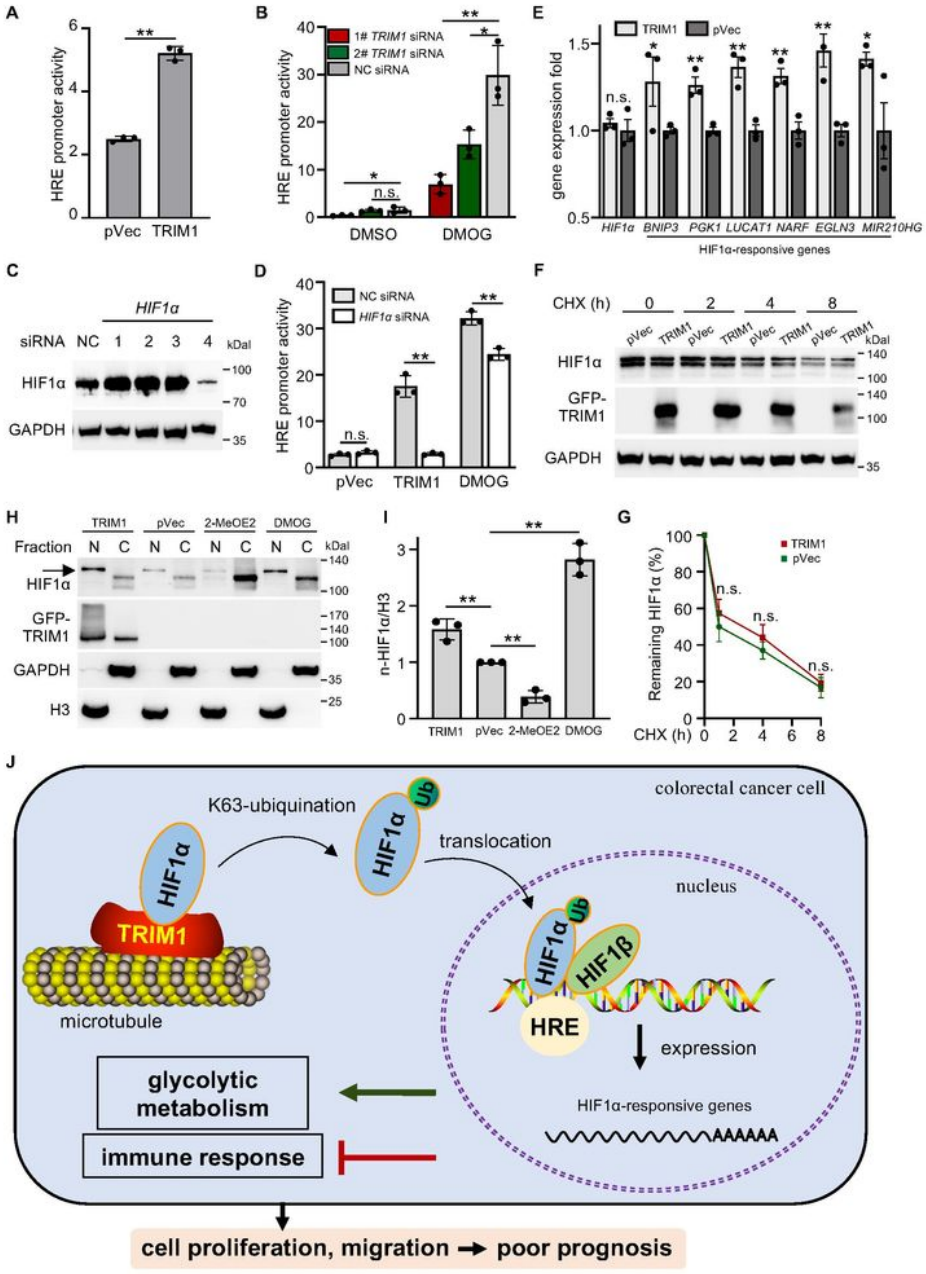

Figure 8

Figure 8

TRIM1 promotes HIF1α activity by accelerating its nuclear translocation

(A). Effects of TRIM1 over-expression on the HIF1α activities. The plasmid construct for GFP-TRIM1 or GFP was co-transfected with the plasmid constructs for HRE-Luc into SW480 cells. HIF1α activity was determined using a luciferase reporter assay.

(B). Effects of TRIM1 knockdown on the HIF1α activities. After transfection of TRIM1 siRNA for 48 h, SW480 cells were transfected with the HRE-Luc plasmid in the presence or absence of DMOG.

(C-D). Effects of HIF1α knockdown on the TRIM1-mediated HRE promoter activity. **(C)** The silencing efficiency of HIF1α siRNA was determined by immunoblotting. **(D)** After transfection of 4# HIF1α siRNA for 48 h, HRE-Luc plasmid was co-transfected with a plasmid construct for GFP-TRIM1 or GFP into SW480 cells. DMOG treatment acted as the positive control.

(E). Effects of TRIM1 expression on the mRNA expression of *HIF1α* and the *HIF1α*-responsive genes. The figure was generated from our transcriptome data.

(F-G). Effects of TRIM1 over-expression on the stability of the endogenous HIF1α. **(F)** SW480 cells were transfected with a plasmid for GFP-TRIM1 or GFP for 18 h and subjected to CHX chase assay and standard immunoblotting analysis with the corresponding antibodies. **(G)** The percentage of the remaining HIF1α was quantitated by determining the ratio of band signal intensity for HIF1α (indicated time)/ HIF1α (0 h) in **(F)** with Image J software.

(H-I). Effects of TRIM1 over-expression on the nucleus distribution of the endogenous HIF1α. **(H)** SW480 cells were transfected with a plasmid for GFP-TRIM1 or GFP for 18 h. Total nucleus (N) and cytosol proteins (C) were fractionated and immunoblotted with the indicated antibodies. 2-ME$(OE)_2$ and DMOG treatment acted as the negative and positive control for this assay. **(I)** The nuclear distribution of HIF1α was quantitated by determining the ratio of band signal intensity for HIF1α (indicated by arrow)/ H3 in **(H)** with Image J software.

Results are as means ± SD from three independent experiments. n.s., not significant, *p<0.05, **p<0.01.

(J). A schematic diagram of this work. TRIM1 expression promotes proliferation and migration of colorectal cancer cells and predicts poor prognosis for CRC patients.

Mechanistically, TRIM1 interacts with HIF1α, catalyzes its K63-linked ubiquitination, and promotes its nuclear translocation. HIF1α in the nuclear then binds the HRE region in the promoter, initiates the expression of downstream genes, promotes cellular metabolism, and attenuates immune response.

Supplementary Files

This is a list of supplementary files associated with this preprint. Click to download.

- 4.SupplementaryFigures.pptx